Electronic Supplementary Material (ESI) for Materials Chemistry Frontiers.

Supporting Information

Novel fluorophore-spacer-receptor to conjugate MWNT and ferrite nanoparticles to design ultra-thin shield to screen electromagnetic radiation

Sourav Biswas[ab], Sujit Sankar Panja[a*] , Suryasarathi Bose[b*]

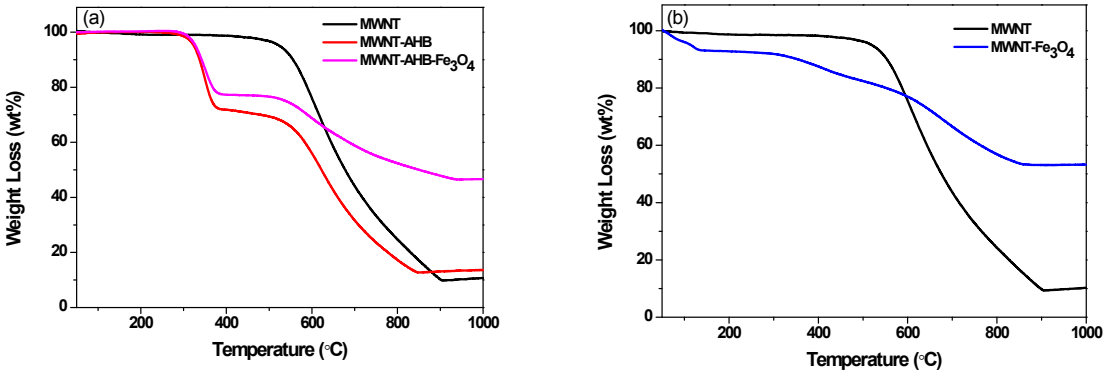

Figure S1: TGA plot of various conjugated nanoparticles in air (a) non-covalent conjugation (b) covalent conjugation.

Here, we have tried to fix the MWNTs concentration as 2 wt% in all the blends. When we prepared MWNT-Fe_3O_4 by covalent conjugation, we have fixed 50/50 weight ratio. At the end of the conjugation we obtained 44% Fe_3O_4 and 46% MWNT as seen from the TGA curves (Figure S1). So during mixing the total amount of filler was fixed at 4 wt% with respect to the total blend, consisting of 2 wt% MWNT and 2 wt% Fe_3O_4. In case of MWNT-AHB- Fe_3O_4 the final yield was 38% Fe_3O_4, 40% MWNT and 22% AHB as obtained from TGA analysis.

High resolution TEM images of various conjugated nanoparticles

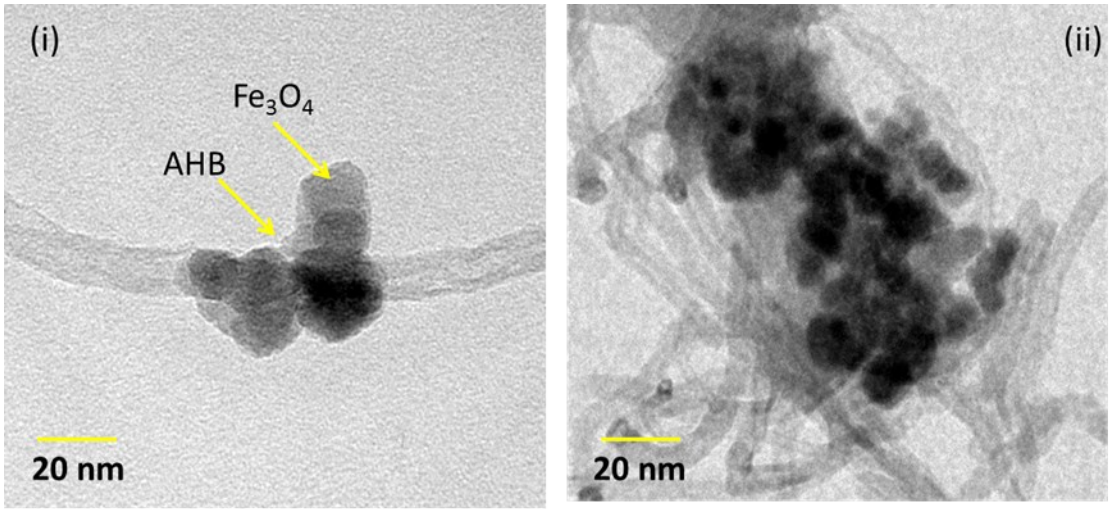

Figure S2: TEM images (i)MWNT-AHB-Fe_3O_4 (ii) MWNT-Fe_3O_4

Monitoring the non-covalent attachment of AHB onto MWNT by UV-vis spectroscopy

The synthesized AHB has extended π-electron cloud associated with the anthracene moiety which can be used to conjugate with the π-electron cloud of MWNTs. The attachment of AHB was further confirmed by UV-vis and fluorescence emission spectroscopy. In general the MWNTs do not show any absorption under UV or fluorescence emission spectroscopy but after non-covalent attachment of AHB, the absorption due to AHB is clearly evident. In general in UV-Vis spectrum, a peak at 255 nm correspond to the π-π^* transition and a peak at 398 nm correspond to n- π^* transition. The unbound AHB molecules were thoroughly washed and the hybrid nanoparticles were monitored using UV-vis spectroscopy (figure S3). The absorption in the hybrid nanomaterials is from the AHB molecules that are non-covalently attached onto the surface of MWNTs as the unbound AHB has been thoroughly washed.

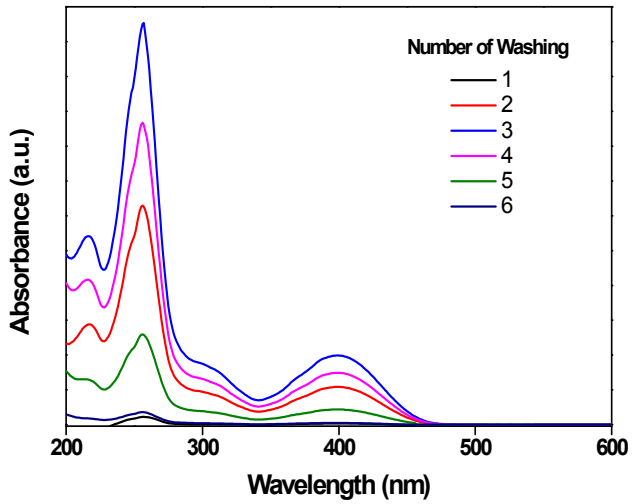

Figure S3: *UV-Vis spectra of successive washing steps to remove unbound AHB from non-covalently modified MWNTs*

Selective localization of hybrid nanoparticles: assessing by DSC

In general, crystallization and melting temperatures are greatly affected by the presence of various rigid nanoparticles and their distribution inside the matrix. So the preferential localization of various nanoparticles in the PVDF phase was further assessed by DSC experiments; changes in the crystallization and melting temperatures of PVDF (table S1 in the supporting information) clearly indicate the presence of hetero nucleating effect of these nanoparticles in the PVDF phase (figure S4).

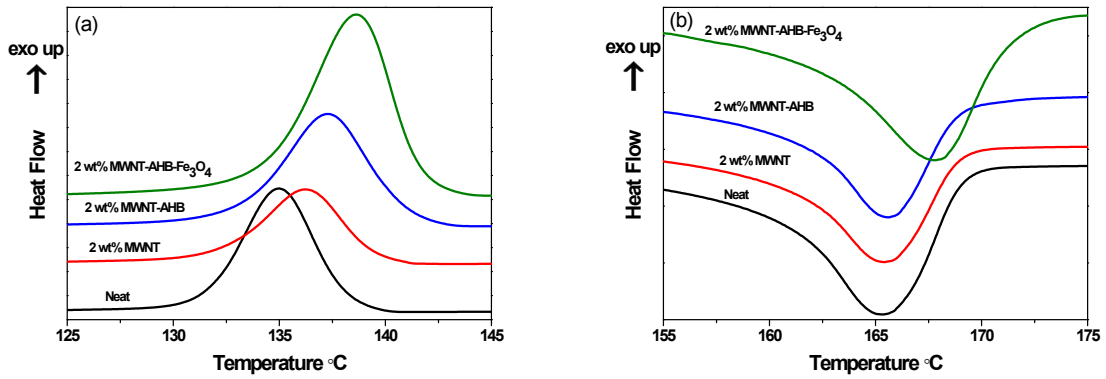

Figure S4: *(a) DSC crystallization curve of various blends (b) DSC melting curve of various blends*

Mechanical properties: effect of efficient dispersion of nanofillers inside the matrix

Interfacial adhesion between the constituents and the phase morphology are the deciding factors on the overall mechanical properties in case of multicomponent system[1-3]. Thermodynamic and chemical incompatibility between the immiscible polymers often results in poor mechanical properties due to poor stress transfer at the interfacial region. Neat 50/50 PC/PVDF blend exhibit much lower mechanical properties than the constituents, which indicates the incompatibility of the system. After the addition of MWNTs, improvement in tensile properties and Young's modulus was observed whereas; elongation at break is sacrificed due to premature failure at the interface originating from the agglomerating MWNTs [figure S5 (a-c)]. Generally, formation of hierarchical microstructure is the important parameters for deciding the mechanical properties of the polymer blend nanocomposites. The mechanical behaviour of blend nanocomposites is contingent on microstructural parameters such as interfacial interaction, localization and state of dispersion of fillers, percolation threshold and the state of dispersion in the matrix. After incorporation of AHB modified MWNTs, improvement in tensile properties and Young's modulus was more prominent due to the better dispersion of nanofillers in the PVDF matrix. However, mechanical properties deteriorate after addition of Fe_3O_4 nanoparticles into the system. Though, conjugation of Fe_3O_4 nanoparticles with MWNTs via non-covalent modification approach showed slight improvement in the properties. Further increase in the concentration of nanoparticles slightly deteriorates the overall properties.

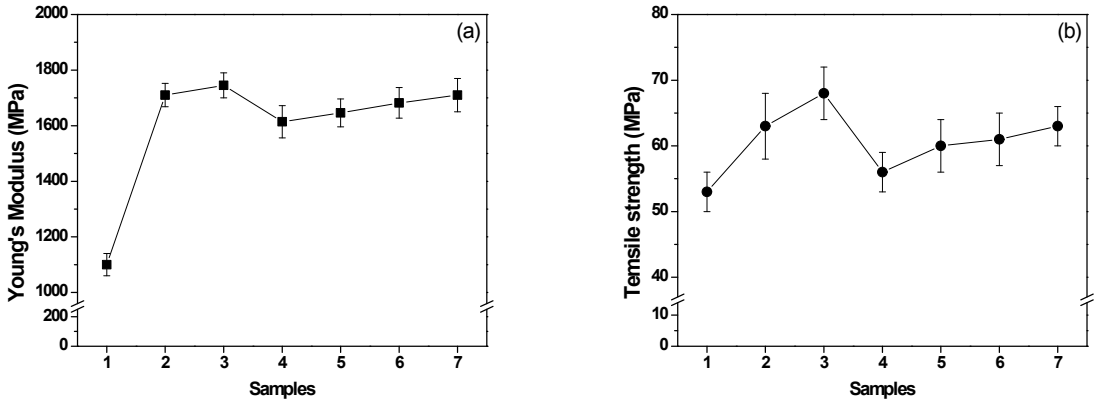

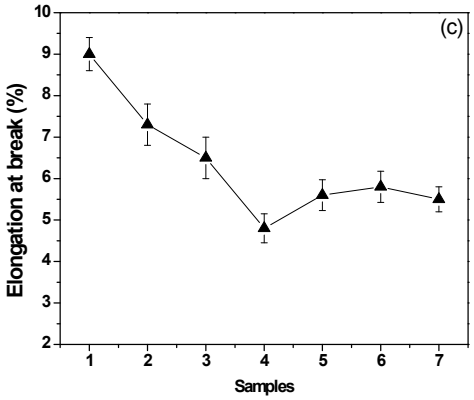

Figure S5: *Mechanical properties of various blends (a) Young's modulus (b) Ultimate tensile strength and (c) % elongation at break, where (1) neat 50/50 blend, (2) 2 wt% MWNT, (3) 2 wt% MWNT-AHB, (4) 2 wt% MWNT + Fe_3O_4, (5) 2 wt% MWNT-Fe_3O_4, (6) 2 wt% MWNT-AHB-Fe_3O_4 and (7) 3 wt% MWNT-AHB-Fe_3O_4 along X-axis.*

Melt rheology: effect of different filler particles

Flow characteristics of the blend were studied by melt rheology, which is an important tool to determine the processability of the nanocomposites. Due to the inter-dependence of viscoelastic properties between the two immiscible polymers, the characteristics flow behavior is complex in nature[4-5]. Figure S6 (a-b) shows the viscoelastic properties of different PC/PVDF blends at 260°C. It is observed that complex viscosity of PVDF is much higher than PC, whereas the 50/50 blends showed complex viscosity in between the two extremes[6]. The complex viscosity of MWNTs filled blends is much higher than the neat blend, particularly at lower frequency, where sufficient time is available for the relaxation of polymer chains. This indicated that the rigid network of MWNTs impedes macromolecular motion in a given flow field. In presence of AHB modified MWNTs, viscosity even raises higher, suggesting more exfoliation of MWNTs network resulting in mesh-like structure that restricts the macromolecular motion. So, the state of dispersion can also be comprehended by viscoelastic properties of the blend. Furthermore, addition of Fe_3O_4 nanoparticles influences the blend complex viscosity by restricting the macromolecular motion to a greater extent. But interestingly, enhancement in complex viscosity is observed greatly only when Fe_3O_4 nanoparticles were attached onto MWNTs surface via chemical conjugation. Now in the case of non-covalent attachment, further enhancement in complex viscosity is achieved suggesting

that the exfoliated network of MWNT is retained with lesser/fewer agglomeration. Further increasing concentration of nanoparticles resulted increasing complex viscosity.

Furthermore, to assess the mechanical response of the blends, dynamic storage modulus was studied and plotted in respect to angular frequency (figure S6 b). Generally the storage modulus increases with the addition of nanoparticles. Generally exfoliated nanoparticles restrict the macromolecular motion resulting in pseudo-solid nature leading to enhanced storage modulus. Further improvement is observed after incorporation of higher amount of filler in the blend.

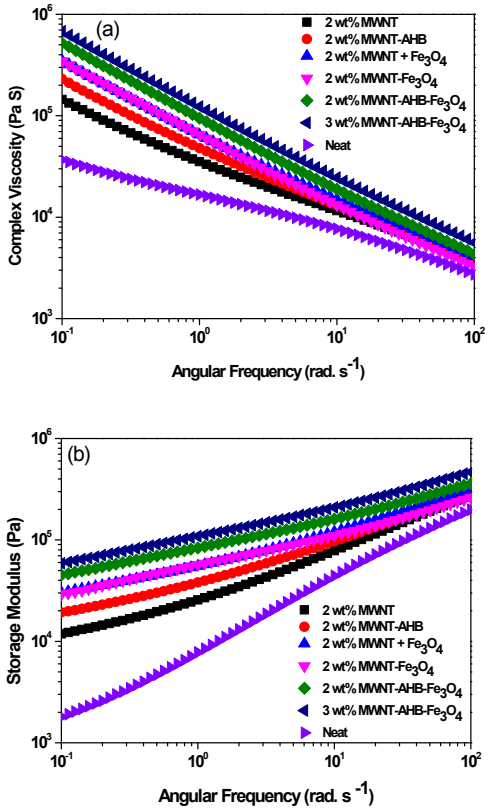

Figure S6: *Melt rheology (a) complex viscosity and (b) storage modulus of various blends*

Table S1: *DSC crystallization and melting temperature of various blends*

Compositions	**Crystallization Temperature (T_c) (°C)**	**Melting Temperature (T_m) (°C)**

50/50 PC/PVDF	135	165
PC/PVDF with 2 wt% MWNT	136	166
50/50 PC/PVDF with 2 wt% MWNT-AHB	137	166
50/50 PC/PVDF with 2 wt% MWNT + Fe_3O_4	139	168

Table S2: *Comparison of shielding efficiency with consisting literatures*

Sr. No.	Matrix	Nanoparticles	Thickness (mm)	SE_T (dB)	RL (dB)	Frequency (GHz)	Reference
1	PVP	MWNT/Fe_3O_4 (40 wt%)	-	-	-35.8	8.56	[7]
2	Polyaniline	Polyaniline coated MWNT/γ Fe_2O_3	2	-34.1	-	2.5	[8]
3	PMMA	MWNT and Fe (catalyst)	-	-27	-	2-12	[9]
4	Epoxy	MWNT (5wt%) /Fe_3O_4 (15wt%)	-	-40	-	13-40	[10]
5	Epoxy	MWNT/ Fe_3O_4 (10 wt%)	1	-	-31.7	13.2	[11]
6	Epoxy	MWNT/ Fe_3O_4 (60 wt%)	5.5	-	-37	2.68	[12]
7	Epoxy	MWNT/ α Fe (20 wt%)	1.2	-	-25	2-18	[13]
8	Epoxy	MWNT/ Fe_3O_4	3.4	-	-41.6	5.5	[14]
9	PVDF/ABS	IL-MWNT (1 wt%) / Fe_3O_4 (2 vol%)	5	-22	-	8-18	[15]
10	PC/SAN	MWNT-grafted-Fe_3O_4 (3 wt%)	5	-32.5	-	8-18	[16]
11	PC/PVDF	MWNT-AHB-Fe_3O_4 (3 wt%)	5	-45	-	8-18	This work
12	PC/PVDF (LBL)	MWNT (3 wt%)+ MWNT-AHB-Fe_3O_4 (3 wt%)	0.9	-60	-	12-18	This work

References

1. Vo, L. T.; Giannelis, E. P., Compatibilizing poly (vinylidene fluoride)/nylon-6 blends with nanoclay. *Macromolecules* **2007,** *40* (23), 8271-8276.
2. Kar, G. P.; Biswas, S.; Bose, S., Simultaneous enhancement in mechanical strength, electrical conductivity, and electromagnetic shielding properties in PVDF–ABS blends containing PMMA

wrapped multiwall carbon nanotubes. *Physical Chemistry Chemical Physics* **2015,** *17* (22), 14856-14865.
3. Aravind, I.; Ahn, K. H.; Ranganathaiah, C.; Thomas, S., Rheology, morphology, mechanical properties and free volume of poly (trimethylene terephthalate)/polycarbonate blends. *Industrial & Engineering Chemistry Research* **2009,** *48* (22), 9942-9951.
4. Pötschke, P.; Fornes, T.; Paul, D., Rheological behavior of multiwalled carbon nanotube/polycarbonate composites. *Polymer* **2002,** *43* (11), 3247-3255.
5. Bose, S.; Bhattacharyya, A. R.; Kulkarni, A. R.; Pötschke, P., Electrical, rheological and morphological studies in co-continuous blends of polyamide 6 and acrylonitrile–butadiene–styrene with multiwall carbon nanotubes prepared by melt blending. *Composites Science and Technology* **2009,** *69* (3), 365-372.
6. Biswas, S.; Kar, G. P.; Bose, S., Tailor made distribution of nanoparticles in blend structure towards outstanding electromagnetic interference shielding. *ACS Applied Materials & Interfaces* **2015**.
7. Zhao, C.; Zhang, A.; Zheng, Y.; Luan, J., Electromagnetic and microwave-absorbing properties of magnetite decorated multiwalled carbon nanotubes prepared with poly (N-vinyl-2-pyrrolidone). *Materials Research Bulletin* **2012,** *47* (2), 217-221.
8. Yun, J.; Kim, H.-I., Electromagnetic interference shielding effects of polyaniline-coated multi-wall carbon nanotubes/maghemite nanocomposites. *Polymer bulletin* **2012,** *68* (2), 561-573.
9. Kim, H.; Kim, K.; Lee, C.; Joo, J.; Cho, S.; Yoon, H.; Pejaković, D.; Yoo, J.-W.; Epstein, A., Electrical conductivity and electromagnetic interference shielding of multiwalled carbon nanotube composites containing Fe catalyst. *Applied Physics Letters* **2004,** *84* (4), 589-591.
10. Liu, Y.; Song, D.; Wu, C.; Leng, J., EMI shielding performance of nanocomposites with MWCNTs, nanosized Fe 3 O 4 and Fe. *Composites Part B: Engineering* **2014,** *63*, 34-40.
11. Zhao, D.-L.; Li, X.; Shen, Z.-M., Preparation and electromagnetic and microwave absorbing properties of Fe-filled carbon nanotubes. *Journal of Alloys and Compounds* **2009,** *471* (1), 457-460.
12. Wen, F.; Zhang, F.; Liu, Z., Investigation on microwave absorption properties for multiwalled carbon nanotubes/Fe/Co/Ni nanopowders as lightweight absorbers. *The Journal of Physical Chemistry C* **2011,** *115* (29), 14025-14030.
13. Che, R.; Peng, L. M.; Duan, X. F.; Chen, Q.; Liang, X., Microwave absorption enhancement and complex permittivity and permeability of Fe encapsulated within carbon nanotubes. *Advanced Materials* **2004,** *16* (5), 401-405.
14. Wang, Z.; Wu, L.; Zhou, J.; Cai, W.; Shen, B.; Jiang, Z., Magnetite nanocrystals on multiwalled carbon nanotubes as a synergistic microwave absorber. *The Journal of Physical Chemistry C* **2013,** *117* (10), 5446-5452.
15. Kar, G. P.; Biswas, S.; Rohini, R.; Bose, S., Tailoring the dispersion of multiwall carbon nanotubes in co-continuous PVDF/ABS blends to design materials with enhanced electromagnetic interference shielding. *Journal of Materials Chemistry A* **2015,** *3* (15), 7974-7985.
16. Pawar, S. P.; Marathe, D. A.; Pattabhi, K.; Bose, S., Electromagnetic interference shielding through MWNT grafted Fe 3 O 4 nanoparticles in PC/SAN blends. *Journal of Materials Chemistry A* **2015,** *3* (2), 656-669.